HHS Public Access

Author manuscript

Proc SPIE. Author manuscript; available in PMC 2016 March 17.

Published in final edited form as:

Proc SPIE. 2015 March 17; 9417: . doi:10.1117/12.2082241.

Subcortical shape and volume abnormalities in an elderly HIV+ cohort

Benjamin S.C. Wade[1], **Victor Valcour**[2], **Edgar Busovaca**[3], **Pardis Esmaeili-Firidouni**[3], **Shantanu H. Joshi**[4], **Yalin Wang**[5], and **Paul M. Thompson**[1]

[1]Imaging Genetics Center, University of Southern California, Marina del Rey, CA, USA

[2]Memory and Aging Center, Department of Neurology University of California, San Francisco, CA, USA

[3]Taub Institute for Research on Alzheimer's Disease and the Aging Brain, Columbia University Medical Center, New York, NY, USA

[4]Ahmanson-Lovelace Brain Mapping Center, Department of Neurology, University of California at Los Angeles, Los Angeles, CA, USA

[5]School of Computing, Informatics, and Decision Systems Engineering, Arizona State University, Tempe, AZ, USA

Abstract

Over 50% of HIV+ individuals show significant impairment in psychomotor functioning, processing speed, working memory and attention [1, 2]. Patients receiving combination antiretroviral therapy may still have subcortical atrophy, but the profile of HIV-associated brain changes is poorly understood. With parametric surface-based shape analyses, we mapped the 3D profile of subcortical morphometry in 63 elderly HIV+ subjects (4 female; age=65.35 ± 2.21) and 31 uninfected elderly controls (2 female; age=64.68 ± 4.57) scanned with MRI as part of a San Francisco Bay Area study of elderly people with HIV. We also investigated whether morphometry was associated with nadir CD4+ (T-cell) counts, viral load and illness duration among HIV+ participants.

FreeSurfer was used to segment the thalamus, caudate, putamen, pallidum, hippocampus, amygdala, accumbens, brainstem, callosum and ventricles from brain MRI scans. To study subcortical shape, we analyzed: (1) the Jacobian determinant (JD) indexed over structures' surface coordinates and (2) radial distances (RD) of structure surfaces from a medial curve. A JD less than 1 reflects regional tissue atrophy and greater than 1 reflects expansion.

The volumes of several subcortical regions were found to be associated with HIV status. No regional volumes showed detectable associations with CD4 counts, viral load or illness duration. The shapes of numerous subcortical regions were significantly linked to HIV status, detectability of viral RNA and illness duration. Our results show subcortical brain differences in HIV+ subjects in both shape and volumetric domains.

Keywords

Shape analysis; HIV; subcortical

1. BACKGROUND

Combined antiretroviral therapy (cART) has vastly improved the quality of life for many people infected with HIV, allowing many of those infected to live to an advanced age. However, even among those receiving long-term, stable cART, upwards of 50% develop symptoms of HIV-associated neurocognitive disorders (HAND) [1, 2]. HAND is characterized by both psychomotor and cognitive impairments in working memory, processing speed, executive function and attention [3–5].

The neurotoxic effects of HIV may preferentially affect periventricular white matter tract integrity, frontal cortices and several subcortical brain structures [6]. The extent of psychomotor dysfunction in HIV has been associated with basal ganglia atrophy [7]. Both volumetric increases (hypertrophy) [8] and reductions (atrophy) [9] have been reported to accompany HAND. As suggested by Hua et al., these differential findings may depend on the stage at which the infections were assessed [10].

While subcortical abnormalities are implicated in HAND, the exact profile of HIV-associated brain abnormalities is not well-understood. More sensitive biomarkers to detect HAND would help clinicians identify which HIV+ subjects are likely to develop neurocognitive disorders, and therefore which patients are in need of early intervention. An important step in characterizing HIV-related neurological abnormalities is to describe local abnormalities in subcortical brain regions. Compared to global volumetric descriptors, surface-based shape features can localize regions of tissue hypertrophy and atrophy.

Here we show the profile of subcortical volumetric and 3D surface-based shape abnormalities in a cohort of 63 elderly HIV+ subjects scanned with structural magnetic resonance imaging (MRI) as part of the UCSF HIV Over 60 Cohort study. To study subcortical shape, we analyzed: (1) the Jacobian determinant (JD) indexed over structures' surface coordinates and (2) radial distances (RD) of structure surfaces from a medial curve. JD maps of a subcortical surface indicate localized atrophy where the determinant is less than 1, and expansion in regions where the JD is greater than 1 [11]. Complementing this, the RD indicates the local "thickness" of the structure.

We additionally tested associations of morphological descriptors with several common HIV clinical indices: nadir CD4+ (nCD4) T-cell count, illness duration, and HIV RNA concentration. We hypothesized that subcortical shape analysis would reveal regions of significant atrophy in HIV+ people relative to matched controls, and that these differences would relate to clinical markers of HIV-related disease.

2. MATERIALS AND METHODS

2.1 Subjects

63 elderly HIV+ subjects (4 women; age=65.35 ± 2.21) and 31 uninfected elderly controls (2 women; age=64.68 ± 4.57) were recruited as part of a San Francisco Bay Area study of elderly people with HIV. HIV+ participants' average nCD4 count was 204.96 ± 154.85 cells/mm^3, with an average illness duration of 20.39 ± 6.31 years. 24 HIV+ participants had

detectable viral RNA concentrations above 50 copies/mm^3. The average viral load among participants with detectable viral RNA was 16,400 ± 76,400 copies/mm^3. All participants provided informed consent to enroll in the study.

2.2 Image acquisition

Each participant underwent a whole-brain magnetic resonance imaging (MRI) anatomical brain scan on a Siemens 3 Tesla TIM Trio scanner with a 12-channel head coil. T1-weighted MP-RAGE sequences (240 × 256 matrix; FOV = 256mm; 160 slices; voxel size = 1.0 × 1.0 × 1.0 mm^3; TI = 900 ms; TR = 2300 ms; TE = 2.98 ms; flip angle = 9°).

2.3 Image segmentation

FreeSurfer was used to segment the following volumes of interest (VOIs) from the raw MRIs: the thalamus, caudate, putamen, pallidum, hippocampus, amygdala, accumbens, brain stem, callosum and lateral and third ventricular spaces. All segmentations were visually inspected to ensure their quality. Figure 1 provides an anatomical template of subcortical volumes inspected using shape analysis.

2.4 Surface parameterization

To derive shape features from a VOI, we converted its binary segmentation to a parametric 3D surface mesh. Each VOI's surface was parametrized using a conformal mapping to a holomorphic 1-form as detailed in [11]. In this way, the conformal parameterization of each surface is mapped to a rectangular Euclidean domain. This method of conformal mapping has the advantage of optimizing the uniformity of the resultant mesh grid [11].

2.5 Morphological features

Three morphological features were measured: (1) Volume, (2) the Jacobian determinant (JD) and (3) radial distance (RD). Volume was computed directly from FreeSurfer for each VOI. JD and RD, the two shape-based features, were not computed for the callosum or ventricular spaces.

In computing the local JD, the Jacobian matrix at each vertex is given by the following: Take φ: $S_1 \rightarrow S_2$ to be the conformal map of the given surface to the rectangular holomorphic 1-form. In a discrete mapping, the derivative map of φ is approximated by the linear mapping between two triangular faces, [ν_1, ν_2, ν_3] $\rightarrow$ [w_1, w_2, w_3], in $\mathbb{R}^2$. The Jacobian matrix, $d\varphi$, is then given by,

$$d\phi = [w_3 - w_1, w_2 - w_1][\nu_3 - \nu_1, \nu_2 - \nu_1]^{-1} \quad \text{(I)}$$

The JD indexed at each vertex is given by the determinant of Jacobian matrix, $d\varphi$. Local surface dilation is indicated by a JD with value greater than 1; conversely a JD with a value less than 1 indicates a region of atrophy.

The second shape feature, RD, was calculated by first computing a 3-dimensional medial core which defined at the structure's local center. The distance of each surface vertex to the

nearest point of the medial core is the radial distance, a measure of the structure's local thickness [12, 13].

2.6 Statistical modeling

Separate multiple linear regression analyses were performed to assess the statistical association between HIV status and other clinical metrics on the various brain measures. The following multiple linear regression model was used:

$$outcome = \beta_0 + \beta_1 \cdot age + \beta_2 \cdot sex + \beta_3 \cdot intracranial\ volume + \beta_4 \cdot main\ effect + \varepsilon \quad \text{(II)}$$

where *outcome* is either volume or the vertex-specific JD or RD and *main effect* is one of HIV status, nCD4 count, viral load or illness duration. Viral load was modeled as a dichotomous variable with participants having more than 50 viral RNA copies/mm^3 having detectable levels; participants below this threshold were considered to have undetectable viral RNA levels.

We controlled for multiple comparisons using the standard false discovery rate (FDR) method with a false-positive rate of 5% ($q = 0.05$) [14]. FDR was performed separately within each class of morphometry features, volume, JD and RD. For the family of volumetric tests, FDR was applied to the set of all subcortical structures, comprising one adjustment per structure. For shape analyses, a separate regression model was fit at each of 15,000 vertices per structure. Here we simply applied FDR within each structure, correcting for 15,000 separate tests within each surface.

3. RESULTS

3.1 HIV status

Volumes of the callosum ($\beta_{dx} = -290$, $t = -2.81$, $p < 0.05$), left pallidum ($\beta_{dx} = -180$, $t = -3.47$, $p < 0.01$), left putamen ($\beta_{dx} = -330$, $t = -2.40$, $p < 0.05$), left thalamus ($\beta_{dx} = -390$, $t = -2.91$, $p < 0.05$) and right thalamus ($\beta_{dx} = -440$, $t = -3.00$, $p < 0.05$) were significantly lower in HIV+ participants. HIV+ subjects exhibited enlarged ventricular spaces relative to controls. The left lateral ($\beta_{dx} = 5100$, $t = 2.88$, $p < 0.05$), right lateral ($\beta_{dx} = 3900$, $t = 2.41$, $p < 0.05$) and third ($\beta_{dx} = 420$, $t = 3.68$, $p < 0.01$) ventricular spaces were all significantly larger in HIV+ participants.

Figure 2 shows regional shape variations between HIV+ and unaffected controls. RD maps show a significantly enlarged central region of the brain stem in HIV+ participants. The RD of the left-hemisphere thalamic surface was significantly decreased in its anterior aspect in HIV. No significant differences were identified by the JD.

3.2 Nadir CD4 count

No significant associations between nCD4 count and volume or shape-based morphometry were observed.

3.3 Viral load

Detectability of viral RNA was not a significant predictor of subcortical volumes among HIV+ participants. However, significant shape-based differences were detected in the left pallidum in association with viral RNA and were observed in both RD and JD maps. We observe anterior atrophy of the left putamen while the posterior region expands in subjects with detectable viral RNA (Figure 3).

3.4 HIV duration

The right pallidal volume was positively associated with illness duration ($\beta_{duration} = 6.3$, $t = 2.43$, $p > 0.05$) but this association did not survive FDR. Corroborating this trend-level effect, both RD and JD maps of the right pallidum revealed significant expansion in its central region in relation to longer illness duration; RD and JD associations both survived FDR (Figure 4).

4. DISCUSSION

Unlike other, more prevalent, forms of dementia, considerably less is known about brain abnormalities in people with HIV and HAND. Cognitive disorders associated with HIV persist, even among patients on stable cART, so it is critical to characterize HIV's affect on key brain regions while also developing biomarkers to track the extent of HIV-associated abnormalities in the central nervous system. With both standard volumetric and surface-based shape descriptors, we identified several brain abnormalities associated with HIV status. Furthermore, we found significant associations between subcortical morphometry and important clinical parameters commonly monitored in HIV+ patients receiving treatment.

We correctly predicted that HIV infection as well as poorer clinical measures associated with HIV would be associated with more severe subcortical atrophy. However, we also observed several unexpected associations: the bilateral pallida was hypertrophied in association with poorer clinical scores; the right hemisphere pallidum with longer illness duration and the left hemisphere pallidum posteriorly with detectable viral RNA concentrations. Notably, this cohort is comprised of exclusively elderly HIV+ participants, many of whom survived infection prior to the advent of modern cART. This raises the possibility that some of these observed differences may result from survivor bias.

Volumetric and shape-based morphometry descriptors each characterized different characteristics of subcortical brain abnormalities in elderly HIV+ participants. Volumetric measures identified a large set of structures differing in size between diagnostic groups, but shape measures alone were able to detect the more subtle associations between clinical measures and subcortical morphometry. Future work will seek to corroborate the observed HIV neurophenotype in other HIV+ cohorts using a similar complement of morphometric descriptors.

ACKNOWLEDGEMENTS

This work was supported in part by NIH 'Big Data to Knowledge' (BD2K) Center of Excellence grant U54 EB020403, funded by a cross-NIH consortium, and by the National Science Foundation Graduate Research Fellowship under Grant No. DGE-0707424.

REFERENCES

1. Cysique L, Maruff P, Brew B. Prevalence and pattern of neuropsychological impairment in human immunodeficiency virus-infected/acquired immunodeficiency syndrome (HIV/AIDS) patients across pre- and post-highly active antiretroviral therapy eras: A combined study of two cohorts. Journal of Neurovirology. 2004; 10:350–357. [PubMed: 15765806]
2. Simioni S, Cavassini M, Annoni JM, et al. Cognitive dysfunction in HIV patients despite long-standing suppression of viremia. AIDS. 2010; 24:1243–1250. [PubMed: 19996937]
3. Brew BJ. Evidence for a change in AIDS dementia complex in the era of highly active antiretroviral therapy and the possibility of new forms of AIDS dementia complex. AIDS. 2004; 18:75–78. [PubMed: 15090832]
4. Heaton RK, Butters N, White DA, Kirson D, Atkinson JH. The HNRC 500-Neuropsychology of HIV infection at different disease stages. J. International Neuropsychological Society. 1995; 1:231–251.
5. Sacktor N, McDermott M, Marder K, Schifitto G, et al. HIV-associated cognitive impairment before and after the advent of combination therapy. Journal of NeuroVirology. 2002; 8:136–142. [PubMed: 11935465]
6. Wiley CA, Achim CL, Christopherson C, Kidane Y, Kwok S, Masliah E, et al. HIV mediates a productive infection of the brain. AIDS. 1999; 13:2055–2059. [PubMed: 10546857]
7. Küper M, Rabe K, Esser S, Gizewski ER, Husstedt IW, Maschke M, et al. Structural gray and white matter changes in patients with HIV. Journal of Neurology. 2011; 258:1066–1075. [PubMed: 21207051]
8. Castelo J, Courtney MG, Melrose RJ, Stern CE. Putamen hypertrophy in nondemented patients with human immunodeficiency virus infection and cognitive compromise. Archives of Neurology. 2007; 64:1275–1280. [PubMed: 17846265]
9. Jernigan TL, Gamst AC, Archibald SL, Fennema-Notestine C, et al. Effects of Methamphetamine Dependence and HIV Infection on Cerebral Morphology. American Journal of Psychiatry. 2005; 162:1461–1472. [PubMed: 16055767]
10. Hua X, Boyle CP, Harezlak J, Tate DF, Yiannoutsos CT, Cohen R, et al. Disrupted cerebral metabolite levels and lower nadir CD4 + counts are linked to brain volume deficits in 210 HIV-infected patients on stable treatment. NeuroImage. Clinical. 2013; 3:132–142. [PubMed: 24179857]
11. Wang Y, Yuan L, Shi J, Greve A, Ye J, Toga AW, et al. Applying tensor-based morphometry to parametric surfaces can improve MRI-based disease diagnosis. NeuroImage. 2013; 74:209–230. [PubMed: 23435208]
12. Apostolova LG, Dinov ID, Dutton RA, Hayashi KM, Toga AW, Cummings JL, et al. 3D comparison of hippocampal atrophy in amnestic mild cognitive impairment and Alzheimer's disease. Brain : a journal of neurology. 2006; 129:2867–2873. [PubMed: 17018552]
13. Apostolova LG, Morra JH, Green AE, Hwang KS, Avedissian C, Woo E, et al. Automated 3D mapping of baseline and 12-month associations between three verbal memory measures and hippocampal atrophy in 490 ADNI subjects. NeuroImage. 2010; 51:488–499. [PubMed: 20083211]
14. Benjamini Y, Hochberg Y. Controlling the false discovery rate- a practical and powerful approach to multiple testing. Journal of the Royal Statistical Society. 1995; 57:289–300.

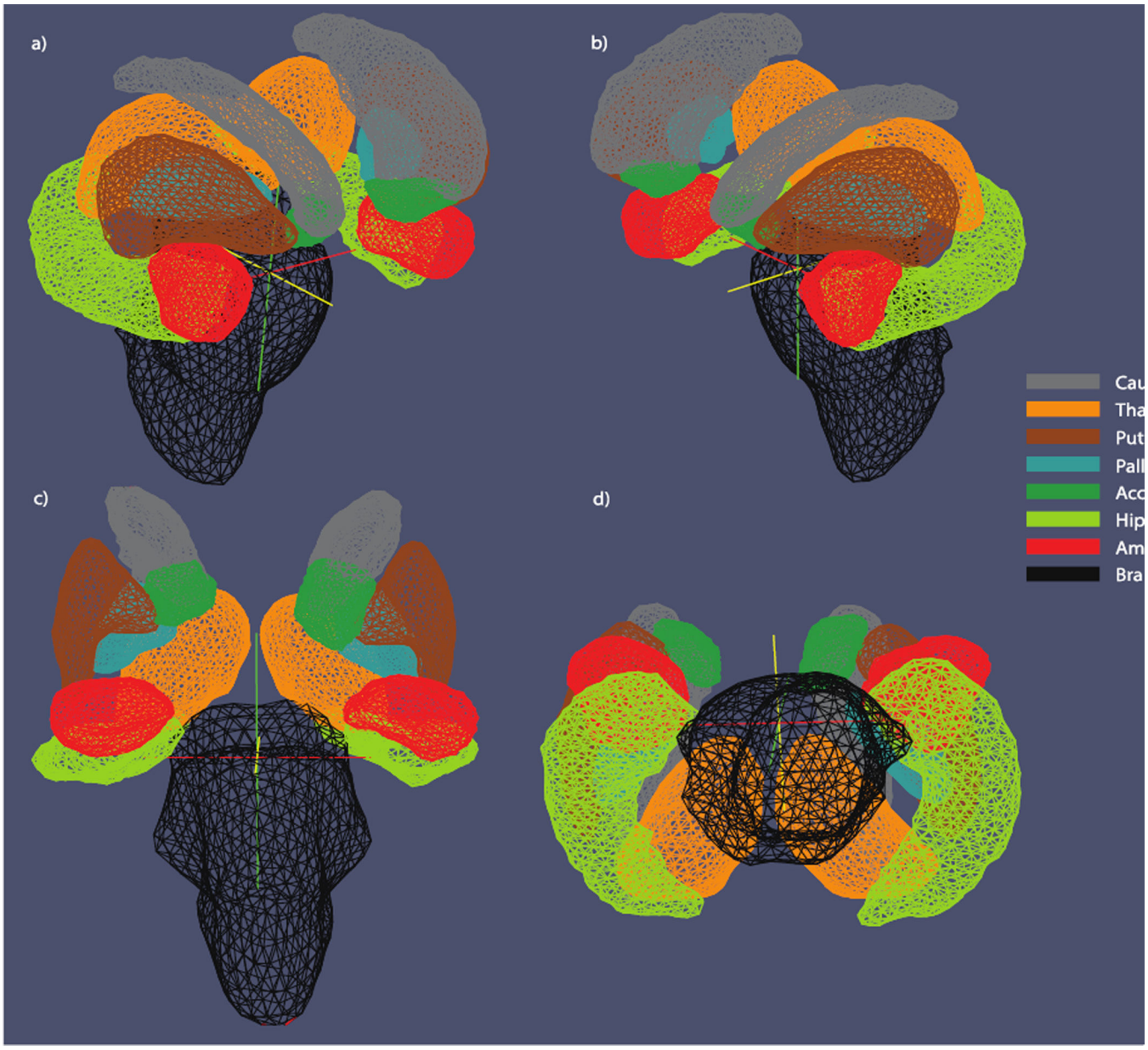

Figure 1.

Subcortical template. Illustration of the eight subcortical surfaces used for shape analysis. Surfaces are illustrated from a) right anterior-lateral, b) left anterior-lateral, c) anterior and d) inferior perspectives.

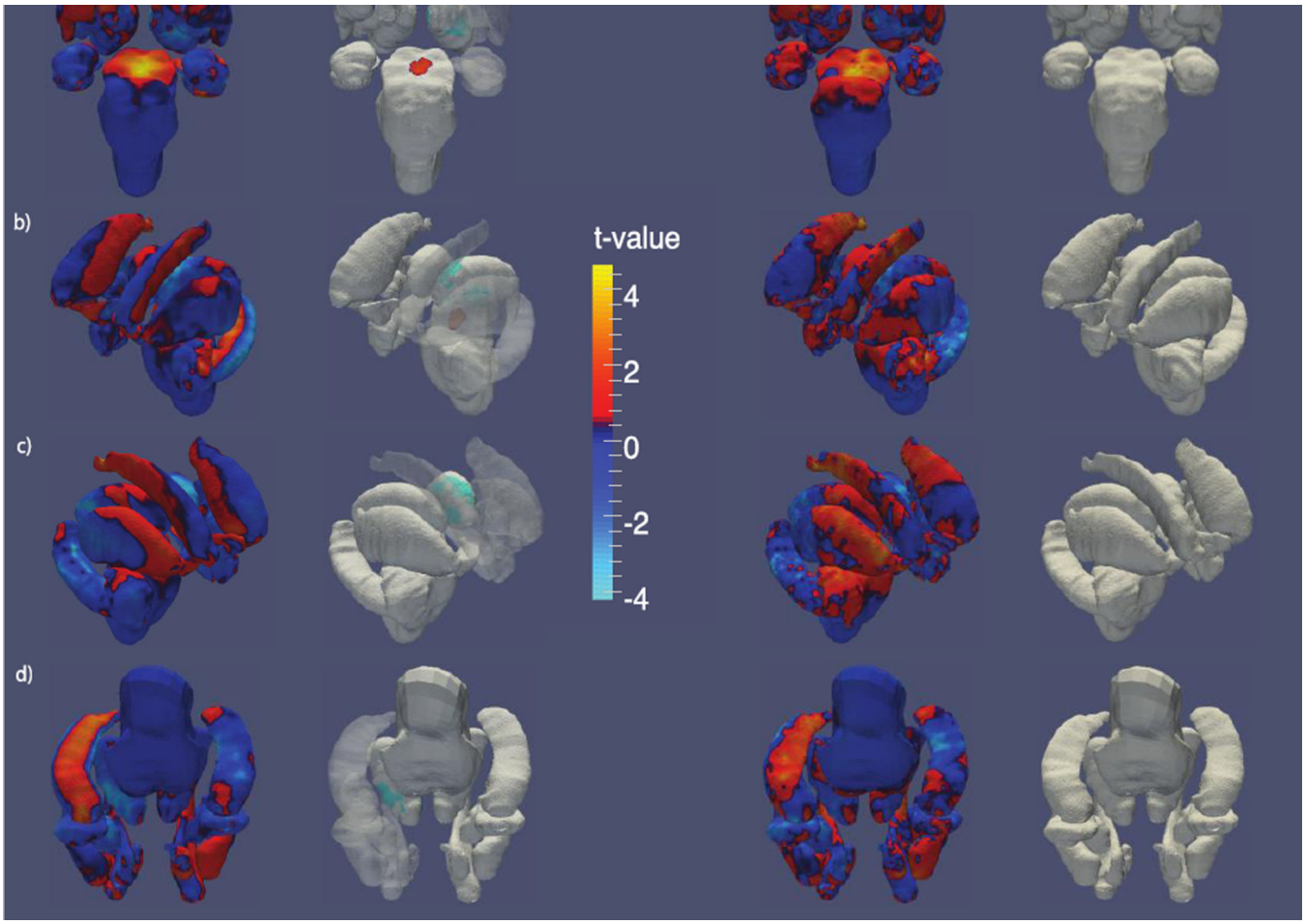

Figure 2.

Shape variation by HIV status. T-value maps of radial distance (left) and the Jacobian determinant (right) from a) anterior, b) left, c) right and d) inferior perspectives. The second and third columns each show t-value maps that have been thresholded to show regions significant after FDR correction.

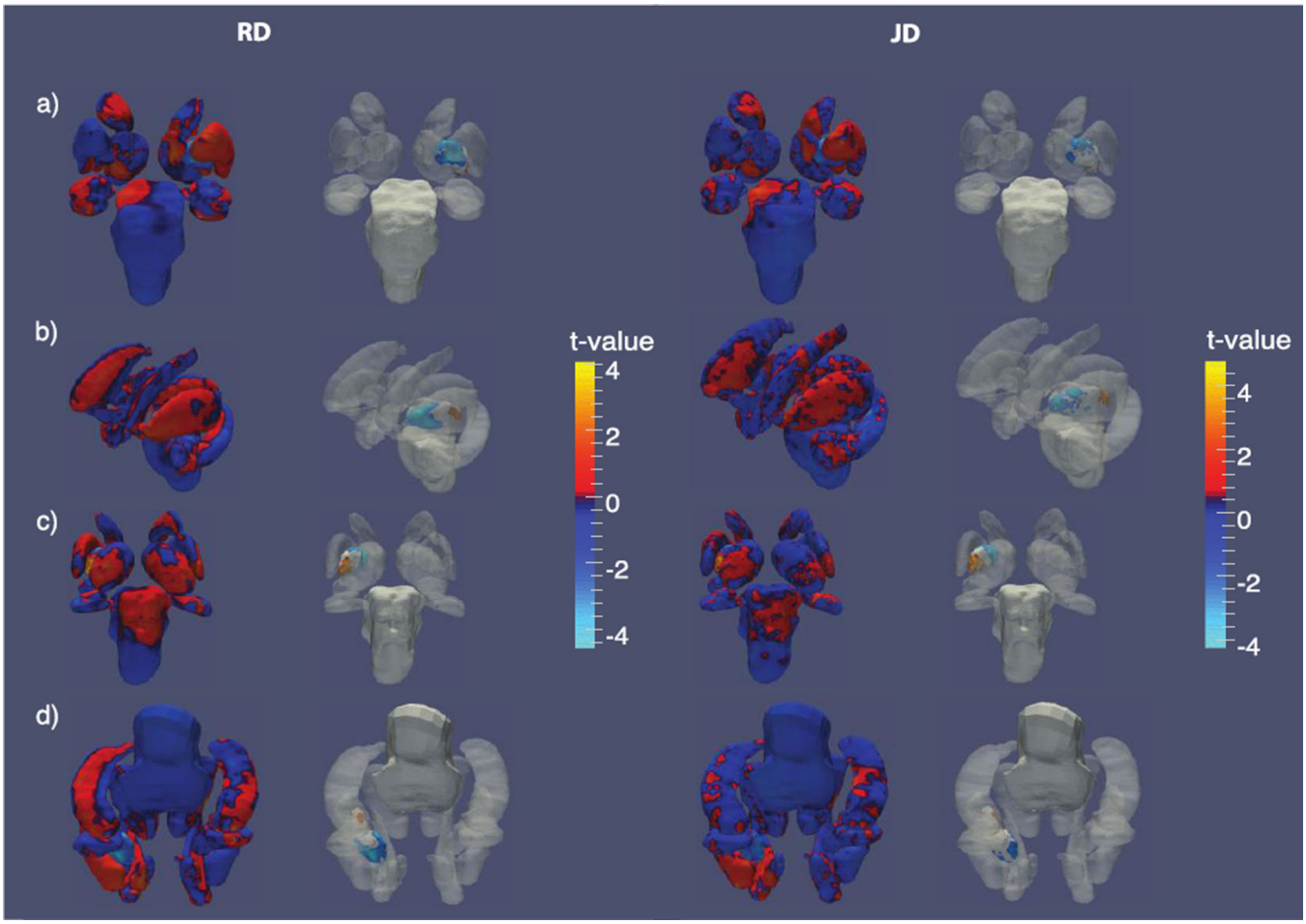

Figure 3.

Shape variation by viral RNA detectability. T-value maps of radial distance (left) and the Jacobian determinant (right) from a) anterior, b) left, c) posterior and d) inferior perspectives. The second and third columns each show t-value maps that have been thresholded to show regions significant after FDR correction.

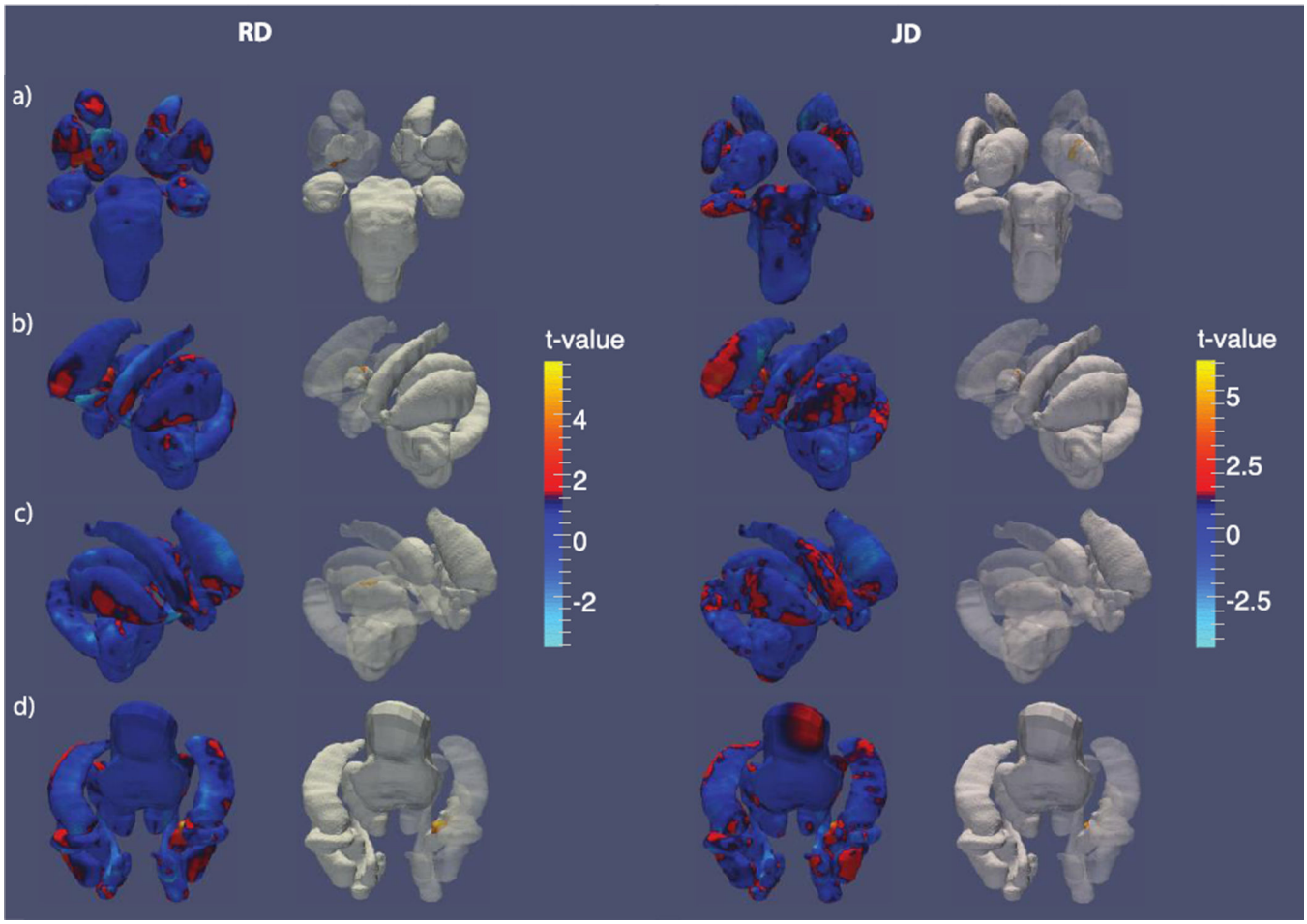

Figure 4.

Shape variation by HIV duration. T-value maps of radial distance (left) and the Jacobian determinant (right) from a) anterior, b) left, c) right and d) inferior perspectives. The second and third columns each show t-value maps that have been thresholded to show regions significant after FDR correction.